A 1-D MANTLE CONDUCTIVITY MODEL DERIVED FROM CHAMP, ØRSTED, AND SAC-C MAGNETIC DATA

A. Kuvshinov[1,2] and N. Olsen[1]

(1) Danish National Space Center, Juliane Maries Vej, 30, 2100 Copenhagen, Denmark, email: alexei@spacecenter.dk, nio@spacecenter.dk

(2) Institute of Terrestrial Magnetism, Ionosphere and Radiowave Propagation, Russian Academy of Sciences, 142190, Troitsk, Moscow region, Russia

ABSTRACT

We present a global 1-D conductivity model which is obtained by analysis of five years (2001-2005) of simultaneous magnetic data from the three satellites Ørsted, CHAMP and SAC-C. After removal of core and crustal fields as predicted by a recent field model we used non-polar scalar and vector observations from the night-side sector. These field residuals are interpreted in terms of a large-scale contribution from the magnetospheric ring current and its induced counterpart. We then derive transfer functions between internal (induced) and external expansion coefficients of the magnetic potential and provide globally-averaged *C*-responses in the period range between 14 hours and 3 months. Inverting the responses yields a 1-D conductivity model which is rather similar to those derived from ground-based data.

1. INTRODUCTION

Temporal variations of the Earth's magnetic field have long been used to infer global conductivity-depth (1-D) profiles of the Earth's mantle, mostly from continental geomagnetic observatories (cf. [1], [2], [3]). In contrast to the data from observatories, which are sparse and irregularly distributed (with only few in oceanic regions), data collected by satellites (such as Magsat, Ørsted, CHAMP and SAC-C) provide full coverage of the Earth's surface. This enables to derive a globally-averaged conductivity profile which is not biased toward continental regions (as is probably the case for most observatory-based models). However, satellite data analysis is more difficult compared to observatory data for two reasons: First, low-orbit satellites move typically with a speed of 7-8 km/s and thus measure a mixture of temporal and spatial changes of the magnetic field. Second, satellites pass over both continents and oceans, and therefore the magnetic satellite data are affected by induction in the oceans [4]. In spite of these difficulties, a number of successful attempts have been made to probe mantle electric conductivity from space ([5], [6], [7], [8], [9]). However, the results of previous satellite data analysis are generally more scattered than those obtained from observatory data. One of the reasons for this is shorter length of the satellite time-series (1 year or less in most previous analyzes), which yields more noisier results compared to an analysis of the several decades of data that are available from ground observatories.

In this paper we estimate *C*-responses (and a 1-D model of mantle conductivity) from a considerably extended satellite data set which includes five years of simultaneous magnetic field recordings from Ørsted, CHAMP and SAC-C satellites.

2. DATA PROCESSING

We use five years (2001-2005) of scalar and vector magnetic field measurements from the Ørsted and CHAMP satellites, and scalar magnetic field measurements from the SAC-C satellite. These data have been processed as follow. First, the core and crustal contributions as predicted by the CHAOS model [10] have been removed from the observations. As part of the CHAOS model, an improved alignment of the CHAMP vector data (i.e., the transformation from the instrument frame to the geocentric frame) was performed; for our study we used these improved CHAMP vector data. In order to reduce the influence of ionospheric currents we only use night-side (magnetic local time between 18:00 and 06:00) and non-polar (dipole latitude equatorward of 50º) data. The thus obtained magnetic field residuals, $\delta\mathbf{B}$, are considered to contain the large-scale contribution from the magnetospheric ring-current and its induced counterpart. These residuals, $\delta\mathbf{B} = -\nabla V$, can be described via a magnetic scalar potential V, which is expanded in spherical harmonics

$$V = a\sum_{n=1}^{N}\left\{\varepsilon_1^0(t)\left(\frac{r}{a}\right)^n + i_1^0(t)\left(\frac{a}{r}\right)^{n+1}\right\}P_n^0(\cos\vartheta), \qquad (1)$$

where a = 6371.2 km is the mean radius of the Earth, ϑ is geomagnetic colatitude, P_n^0 are the associated Schmidt semi-normalized Legendre functions of degree n and order 0, ε_1^0 and i_1^0 are the Gauss coefficients describing sources internal and external to the Earth, respectively, and N is the maximum degree of the expansion. For this representation we assume an axially symmetric field (in dipole geometry), i.e. the expansion

only contains spherical harmonics of order $m = 0$.

Estimation of the coefficients on an orbit-by-orbit basis is the usual approach when analyzing single satellite data. In this case the sampling interval of the recovered time series of ε_1^0 and i_1^0 is given by the orbit period (approximately 1.5 hours). This approach is, however, not suitable for the analysis of simultaneous data from more than one satellite due to the lack of a common natural time basis (e.g., the satellites do not pass the equator simultaneously). This difficulty can be overcome by parameterizing the time dependency of the coefficients by cubic *B*-splines. This was previously done by [8], and the present study is an extension of this work, using essentially the same approach but a much larger data set. Spacing of the spline knots is 4 hours.

If available we used all three vector components; scalar data were only used if vector data were not available. Sampling interval of all data was 1 minute. We estimated 4 external expansion coefficients, ε_1^0, and 4 corresponding induced coefficients i_1^0 ($n = 1-4$) using iteratively reweighted least squares with Huber weights [11]. As expected, the coefficients ε_1^0 and i_1^0 are the largest; only these coefficients will be used in the following analysis. However, we include an estimation of the higher degree terms in order to obtain unbiased values for the degree-1 coefficients ε_1^0 and i_1^0.

3. RESPONSE FUNCTIONS ESTIMATION

1-D electromagnetic (EM) response functions are estimated as the frequency dependent transfer function $Q(\omega)$ between the Fourier transformed time series ε_1^0 and i_1^0

$$i_1^0(\omega) = Q_1(\omega)\,\varepsilon_1^0(\omega), \qquad (2)$$

where ω is angular frequency. We used the section averaging approach [3] to estimate $Q_1(\omega)$. For comparison we also estimated the responses using the multi-taper spectral estimation technique [12] and found good agreement when using a fixed number (20) of tapers. $Q_1(\omega)$ is finally transformed to the *C*-response [13] by means of

$$C(\omega) = \frac{a}{2}\,\frac{1-2Q_1(\omega)}{1+Q_1(\omega)}. \qquad (3)$$

Tab. 1 lists our response estimates and squared coherency, coh^2, between i_1^0 and ε_1^0. Fig. 1 shows these *C*-responses estimates together with results obtained by other studies. The values of [3] are average responses from European observatory data; those of [14] are essentially the responses of [15] corrected for the ocean effect. (The initial responses of [15] have been derived from electric potential variations observed with submarine cables across the North Pacific Ocean, and magnetic field variations observed at nearby coastal observatories.) Finally, the values of [9] are global response functions estimated from Magsat satellite data.

Table 1. C-responses (in km) and squared coherencies coh^2 *for 17 periods (in seconds), derived from 5 years of CHAMP, Ørsted and SAC-C magnetic data.*

T	Re *C*	Im *C*	δC	coh^2
50700	248	-266	24	0.83
71600	407	-268	28	0.83
100900	496	-221	31	0.83
142300	614	-162	27	0.90
200600	685	-149	30	0.91
282900	734	-105	28	0.96
398900	728	-134	37	0.93
562400	764	-134	42	0.93
793000	779	-187	50	0.93
1118100	801	-242	56	0.94
1576600	831	-259	62	0.93
2222000	892	-294	97	0.92
3134400	898	-239	148	0.86
4419500	1130	-281	194	0.83
6231500	1155	-237	201	0.91
8786300	1323	-269	253	0.84
12388700	1310	-321	337	0.82

The responses are rather similar in the period range between 2 and 20 days, but reveal systematic differences outside this interval. At periods greater than one month, the *C*-responses of [9] correspond to higher conductivity in the lower mantle, compared to the other presented responses. For periods less than a few days the responses of [14] exhibits a behaviour that suggests a rather resistive upper part of the mantle. On the contrary, our new satellite *C*-responses suggest increased conductivity at shallow depth, most probably due to induction in the oceans. A possible way to correct for the ocean effect is discussed in [16].

4. 1-D CONDUCTIVITY MODEL ESTIMATION

Using the limited memory quasi-Newton (QN) algorithm of [17] we derived spherical 1-D conductivity models from the various *C*-response estimates. The spherical layer thicknesses increase with depth as a geometric series of step size 1.1, starting from a top layer thickness of 0.5 km. Each model terminates with a infinitely conducting core at a depth of 2900 km. To efficiently calculate the misfit gradients we obtained analytical expressions for the derivatives of the 1-D response functions (see Appendix). The solution is stabilized by requiring minimum first derivative of

log(conductivity) with respect to log(depth).

For the considered 1-D problem this QN algorithm produces results that are very similar to those obtained with the Occam algorithm of [18]. However, we prefer to use the QN approach since it allows for imposing constraints on the model parameters (in our case log(conductivity)). In addition, we believe that the limited memory QN scheme is suitable for the (efficient) solution of the three-dimensional (3-D) inverse problems (cf. [19]) that we plan to perform in future.

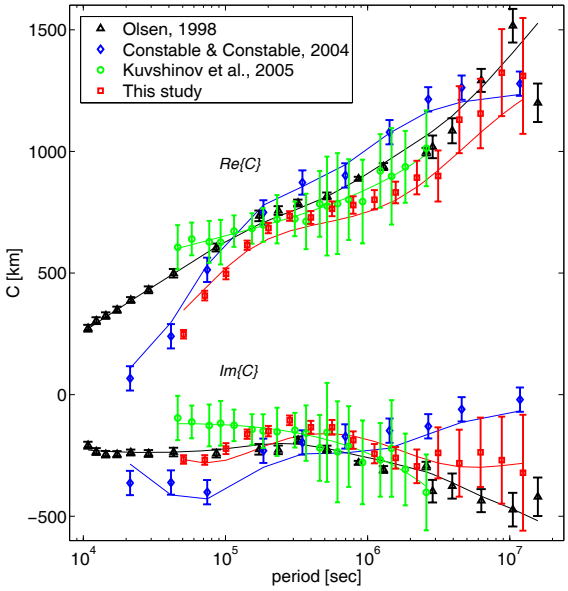

Figure 1. Satellite C-responses of this study together with results obtained by other studies. Symbols refer to response estimates, whereas the solid lines present responses of the respective models shown in Fig. 2.

The regularization parameter α of our inversion scheme describes the trade-off between model misfit χ^2 and model smoothness. α is found by means of a cooling approach; starting from a large value of α, several inversions are performed with decreasing α until the model χ^2 reaches its target value (which depends on the assumed data errors). However, due to different ways of calculating data errors when deriving the various data sets we used a heuristic approach and selected α such that similar model smoothness is obtained.

Fig. 2 shows the result of the inversion. Below 400 km depth the conductivity obtained from our satellite *C*-responses is rather similar to that derived from ground-based data. All models show a monotonic increase of conductivity from 0.03-0.08 S/m at z = 400 km depth to 1 - 2.5 S/m at z = 900 km depth. However, conductivity based on our new satellite responses is slightly (but systematically) higher at all depths below 400 km.

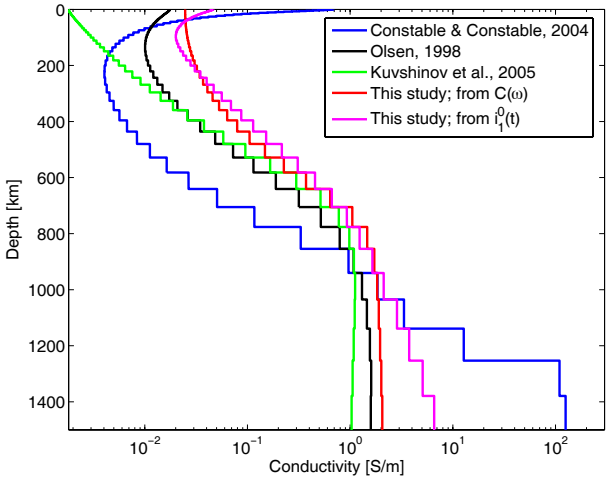

Figure 2. 1-D conductivity models derived from the various data sets shown in Fig. 1.

Below 900 km the conductivities recovered from ground-based and our satellite responses are almost constant, as opposed to the large increase reported by [9]. To investigate this further, we inverted our satellite data in the time domain by estimating a 1-D conductivity model by direct inversion of 5 years of time series of the induced coefficients, $i_1^0(t)$, rather than the transfer function $C(\omega)$. The thus obtained conductivity profiles appeared to agree well with those obtained from an inversion of the *C*-responses (see Fig. 2).

We also looked at the RMS misfit between the observed time series, $i_1^0(t)$, and predictions, $i_1^{0,pred}(t) = Q_1 * \varepsilon_1^0(t)$ where "*" stands for convolution, for various conductivity profiles from which we calculated the convolution kernel Q_1. All described profiles gave misfit values between RMS = 2.07 nT and 2.11 nT; only the conductivity model of [9] resulted in a larger misfit (RMS = 2.38 nT), which indicates that this model is less compatible with our satellite time series.

Above 400 km our conductivity model is more conducting compared to the other profiles. Note, however that correction of the data for induction in the oceans removes this difference [16].

5. CONCLUSIONS

We estimated *C*-responses in the period range between 14 hours and three months from five years (2001-2005) of simultaneous magnetic data collected by the three

satellites Ørsted, CHAMP and SAC-C.

Interpreting these responses in terms of mantle conductivity leads to values that are similar to those derived from ground-based data, at least for depths greater than 400 km. All models show a monotonic increase of conductivity from 0.03-0.09 S/m at z = 400 km to 1 - 2.5 S/m at z = 900 km. However, our new 1-D model is slightly (but systematically) more conducting at all depths below 400 km.

Inversion of our data does not favour an increase in conductivity (up to 100 S/m or higher) at depths greater than 900 km, as reported by [9] from an analysis of Magsat satellite data.

At periods shorter than 7 days, satellite responses are most probably influenced by induction in the oceans and correcting the data for this effect is needed. A possible way to correct the data for the ocean effect is discussed in [16].

The results reported here are based on the assumption that mantle conductivity only varies with depth. Work is ongoing to detect lateral variations of mantle conductivity. The results of this effort will be the subject of a forthcoming publication.

6. ACKNOWLEDGMENTS

We are grateful to Bob Parker and Cathy Constable for providing the multi-taper code. The Ørsted and SAC-C Projects were made possible by extensive support from the Danish Government, NASA, ESA, CNES, DARA and CONAE. The support of the CHAMP mission by the German Aerospace Center (DLR) and the Federal Ministry of Education and Research (BMBF) is gratefully acknowledged. This work is supported in part by the Russian Foundation for Basic Research under grant No. 06-05-64329-a.

7. REFERENCES

1. Schmucker U., *Landolt-Börnstein, New Series*, 5/2b, pp. 370-397, Springer-Verlag, Berlin-Heidelberg, 1985.
2. Schultz A. and Larsen J., *Geophys. J. R. astr. Soc.*, V. 88, 733-761, 1987.
3. Olsen N., Geophys. J. Int., V. 133, 298-308, 1998.
4. Kuvshinov A. and Olsen. N., *Earth observation with CHAMP: Results from three years in orbit*, edited by C. Reigber, H. Lühr, P. Schwintzer and Wickert., pp 352-359, 2005.
5. Didwall E. M., J. Geophys. Res., V. 89, 537-542, 1984.
6. Oraevsky V. N. et al., J. Geomag. Geoelectr., V. 45, 1415-1423, 1993.
7. Olsen N., Surveys in Geophysics, V. 20, 309-340, 1999.
8. Olsen N. et al., First CHAMP mission results for gravity magnetic and atmospheric studies, edited by C. Reigber, H. Lühr and P. Schwintzer, pp. 245-250, 2002.
9. Constable S. and Constable C., Geochemistry, Geophysics, Geosystems, V.5, doi:10.1029/2003GC000634, 2004.
10. Olsen N. et al., Geophys. J. Int., in press, 2006.
11. Olsen N., Geophys. J. Int., V. 149, 454-462, 2002.
12. Riedel K. and Sidorenko A., IEEE Trans. Signal Process., V. 43, 188-195, 1995.
13. Weidelt P., Z. Geophys., V. 38, 257-289, 1972
14. Kuvshinov A. et al., Geophys. J. Int., V. 160, 505-526, 2005.
15. Utada H. et al., Geophys. Res. Lett., V.30, doi: 10.1029/2002GL016092, 2003
16. Kuvshinov A. and Olsen N., Geophys. Res. Lett., submitted, 2006.
17. Byrd R. et al., SIAM J. Scientific Computing, V.5, 1190-1208, 1995.
18. Constable S. et al., Geophysics, V. 52., 289-300, 1987.
19. Newman G. and Boggs. P., Inverse Problems, V. 20., 151-170, 2004.
20. Fainberg E. B. et al., Geophys. J. Int., V. 102, 273-281, 1990.
21. Kuvshinov A. et al., *3D Electromagnetics*, edited by M. S. Zhdanov and P. E. Wannamaker, Chap. 3, pp. 43–54, Elsevier, New York, 2002.

APPENDIX

We obtain in the Appendix analytical expressions for the derivatives of the 1-D response functions with respect to conductivities. We assume a spherical symmetric (1-D) conductivity section consisting of N shells; within each shell the conductivity varies as

$$\sigma(r) = \sigma_l \left(\frac{r_l}{r} \right)^2, \qquad \text{(A1)}$$

where $r_{l+1} < r \le r_l$, $r_1 = a$, $r_{N+1} = 0$. The radial dependency of (A1) (e.g. [20]) is chosen to simplify the calculations. Since N can be taken as large as necessary, (A1) allows essentially the approximation of any radially symmetric conductivity section. For such a section the recurrence for calculating the response function (admittance), $Y_l \equiv Y(r = r_l)$, is given by the expression [21]

$$Y_l = \frac{1}{q_l} \frac{q_{l+1} Y_{l+1} (b_l - 0.5\tau_l) + b_l^+ b_l^- \tau_l}{(b_l + 0.5\tau_l) + q_{l+1} \tau_l Y_{l+1}}, \qquad \text{(A2)}$$

where $l = N-1, N-2, ..., 1$, $Y_N = -\dfrac{b_N^+}{q_N}$ and

$$q_l = i\omega\mu_o r_l, \quad b_l = \left\{\left(n+\frac{1}{2}\right)^2 - i\omega\mu_o\sigma_l r_l^2\right\}^{\frac{1}{2}},$$

$$b_l^{\pm} = b_l \pm \frac{1}{2}, \quad \tau_l = \frac{1-\eta_l^{2b_l}}{1+\eta_l^{2b_l}}, \quad \eta_l = \frac{r_l}{r_{l+1}}.$$

Here μ_o is the vacuum magnetic permeability, $i = \sqrt{-1}$, $\omega = 2\pi/T$ is angular frequency, T is period; we assume also that the time factor is $e^{-i\omega t}$. Note that C_n at the Earth's surface and Q_n are connected to Y_1 as

$$C_n = -1/i\omega\mu_o Y_1, \tag{A3}$$

and

$$Q_n = \frac{n}{n+1}\frac{i\omega\mu_o a Y_1 + n + 1}{i\omega\mu_o a Y_1 - n}. \tag{A4}$$

By representing Eq. (A2) as

$$Y_l = f(\sigma_l, f\{\sigma_{l+1}, f[\sigma_{l+1}, ..., f(\sigma_{N-1}, Y_N)]...\}), \tag{A5}$$

and using the chain rule we can write $\partial Y_l/\partial\sigma_m$ as

$$\frac{\partial Y_l}{\partial\sigma_m} = \frac{\partial Y_l}{\partial Y_{l+1}}\frac{\partial Y_{l+1}}{\partial Y_{l+2}}...\frac{\partial Y_m}{\partial\sigma_m}, \quad m = 1, 2, ..., N, \tag{A6}$$

where

$$\frac{\partial Y_\gamma}{\partial Y_{\gamma+1}} = \frac{q_{\gamma+1}}{q_\gamma}\frac{b_\gamma^2 - (b_\gamma^+ b_\gamma^- + 0.25)\tau_\gamma^2}{\{(b_\gamma + 0.5\tau_\gamma) + q_{\gamma+1}\tau_\gamma Y_{\gamma+1}\}^2}, \tag{A7}$$

with $\gamma = l, l+1, ..., N-1$, and where

$$\frac{\partial Y_m}{\partial\sigma_m} = -\frac{(q_{m+1}Y_{m+1} + 0.5)\tau_m^2 + \tau_m b_m}{r_m^{-1}(b_m + \tau_m(0.5 + q_{m+1}Y_{m+1}))^2}$$

$$-\frac{\left(\frac{\tau_m}{2b_m} + \frac{2\eta_m^{2b_k}\ln\eta_m}{(1+\eta_m^{2b_k})^2}\right)\left(q_{m+1}Y_{m+1}(q_{m+1}Y_{m+1}+1) - b_m^+ b_m^-\right)}{r_m^{-1}(b_m + \tau_m(0.5 + q_{m+1}Y_{m+1}))^2}. \tag{A8}$$

Note also that $\partial Y_N/\partial\sigma_N = r_N/2b_N$. For $\partial Q_n/\partial\sigma_m$ and $\partial C_n/\partial\sigma_m$ we have

$$\frac{\partial Q_n}{\partial\sigma_m} = \frac{\partial Q_n}{\partial Y_1}\frac{\partial Y_1}{\partial\sigma_m}, \qquad \frac{\partial Q_n}{\partial Y_1} = -\frac{n}{n+1}\frac{(2n+1)q_1}{(q_1Y_1 - n)^2}, \tag{A9}$$

$$\frac{\partial C_n}{\partial\sigma_m} = \frac{\partial C_n}{\partial Y_1}\frac{\partial Y_1}{\partial\sigma_m}, \qquad \frac{\partial C_n}{\partial Y_1} = \frac{1}{i\omega\mu_o (Y_1)^2}. \tag{A10}$$

Finally, derivatives $\partial i_1^0(t)/\partial\sigma_m$ (that are needed to invert $i_1^0(t)$) can be obtained from

$$\partial i_1^0(\omega)/\partial\sigma_m = \frac{\partial Q_n}{\partial\sigma_m}\varepsilon_1^0(\omega). \tag{A11}$$

by means of an inverse Fourier transform.